

Time-dependent plumes and jets with decreasing source strengths

By M. M. SCASE¹, C. P. CAULFIELD^{2,1},
S. B. DALZIEL¹ AND J. C. R. HUNT³

¹Department of Applied Mathematics and Theoretical Physics, University of Cambridge,
Centre for Mathematical Sciences, Wilberforce Road, Cambridge CB3 0WA, UK

²BP Institute, University of Cambridge, Madingley Road, Cambridge CB3 0EZ, UK

³Centre for Polar Observation and Modelling, Department of Space and Climate Physics, Pearson
Building, University College London, Gower Street, London WC1E 6BT, UK

(Received 14 November 2005 and in revised form 8 March 2006)

The classical bulk model for isolated jets and plumes due to Morton, Taylor & Turner (*Proc. R. Soc. Lond. A*, vol. 234, 1956, p. 1) is generalized to allow for time-dependence in the various fluxes driving the flow. This new system models the spatio-temporal evolution of jets in a homogeneous ambient fluid and Boussinesq and non-Boussinesq plumes in stratified and unstratified ambient fluids.

Separable time-dependent similarity solutions for plumes and jets are found in an unstratified ambient fluid, and proved to be linearly stable to perturbations propagating at the velocity of the ascending plume fluid. These similarity solutions are characterized by having time-independent plume or jet radii, with appreciably smaller spreading angles ($\tan^{-1}(2\alpha/3)$) than either constant-source-buoyancy-flux pure plumes (with spreading angle $\tan^{-1}(6\alpha/5)$) or constant-source-momentum-flux pure jets (with spreading angle $\tan^{-1}(2\alpha)$), where α is the conventional entrainment coefficient. These new similarity solutions are closely related to the similarity solutions identified by Batchelor (*Q. J. R. Met. Soc.*, vol. 80, 1954, p. 339) in a statically unstable ambient, in particular those associated with a linear increase in ambient density with height.

If the source buoyancy flux (for a rising plume) or source momentum flux (for a rising jet) is decreased generically from an initial to a final value, numerical solutions of the governing equations exhibit three qualitatively different regions of behaviour. The upper region, furthest from the source, remains largely unaffected by the change in buoyancy flux or momentum flux at the source. The lower region, closest to the source, is an effectively steady plume or jet based on the final (lower) buoyancy flux or momentum flux. The transitional region, in which the plume or jet adjusts between the states in the lower and upper regions, appears to converge very closely to the newly identified stable similarity solutions. Significantly, the predicted narrowing of the plume or jet is observed. The size of the narrowing region can be determined from the source conditions of the plume or jet. Minimum narrowing widths are considered with a view to predicting pinch-off into rising thermals or puffs.

1. Introduction

The analysis of turbulent plumes and jets by Morton, Taylor & Turner (1956, herein referred to as MTT56), has been widely applied (with 639 citations, 127 in the last five years alone, despite the uncertain physical justification of its basic entrainment assumption, and the recognition that in certain circumstances it is not valid). This

is testimony to the ongoing relevance of their model and its suitability for current applications. MTT56 used their models to predict steady Boussinesq (Boussinesq 1903) plume and jet shapes and their respective velocities, i.e. plumes where density variations are sufficiently small that they are insignificant for the flow's inertia, and only play a role in the buoyancy. It was demonstrated that Boussinesq point-source plumes (i.e. continuous sources of buoyancy alone) rising through a homogeneous background fluid had conical envelopes and their mean centreline velocities scaled as $z^{-1/3}$, where z is the vertical distance from the source. In such flows the buoyancy flux in the plume is constant with height. Jets (i.e. continuous sources of momentum, but zero buoyancy) were also demonstrated to have conical envelopes (although with a different angle of spread) and had mean centreline velocities which scaled as z^{-1} . (These similarity solutions had been identified earlier and independently by Zeldovich 1937.) The influence of stable ambient stratification on height of rise due to the fact that the buoyancy flux is decreasing was also considered in MTT56.

Further advances in their model have been made in recent years. Rooney & Linden (1996) and Woods (1997) considered steady non-Boussinesq plumes and were able to derive expressions for the plume shape and velocity. Caulfield & Woods (1998) considered a family of steady, yet unstable, similarity solutions for plumes in non-uniformly stratified fluids. Several authors (e.g. Caulfield 1991; Caulfield & Woods 1995; Hunt & Kaye 2001, 2005) have considered non-pure plumes (i.e. general sources of volume flux, momentum flux and buoyancy flux). Non-pure plumes adjust over some finite distance towards pure plume balance where the volume flux and momentum flux are related in such a way that they appear to be associated with a source providing buoyancy alone. This asymptotic pure plume is then traced back to an effective 'virtual origin' that is in general distinct from the actual source location. The location of this virtual origin depends on whether the source is 'forced', and thus has an excess of momentum flux compared to a source in pure plume balance, or 'lazy', and thus has a deficiency of momentum flux compared to a source in pure plume balance.

Hunt & Kaye (2005) also considered the effect of a constant-buoyancy release with height, identifying a new class of steady similarity solutions, which had a slightly narrower spreading rate than the conventional pure plume of MTT56. Bhat & Narasimha (1996) considered an experimental analogue, where an initially neutrally buoyant jet was subjected to volumetric heating between two planes perpendicular to the axis of symmetry. They observed that the rate of spread of the jet reduced 'drastically'. Carey, Sigurdsson & Sparks (1988), Woods & Caulfield (1992) and Caulfield & Woods (1995) considered the related situation where the buoyancy flux increased with height due to different processes (either particle fallout or non-monotonic mixing) modelling the behaviour of volcanic eruption clouds. They also observed narrowing of the plume as the flow adjusted.

However, there has been no previous study of the behaviour of a system where the source conditions reduce in time, a situation that is much more likely to occur in nature (e.g. rising thermals and plumes generated in deserts or descending heavy salt plumes under sea ice). Motivated by the study of Hunt *et al.* (2003), we consider this situation in the present paper. Critically, we shall assume that both an entrainment assumption and an assumption of self-similarity at all heights can be made (see Turner 1986). This requires that the time scale over which the bulk characteristics of the plume change is sufficiently long compared to the characteristic time scales of the turbulent processes which are being parameterized by the entrainment coefficient.

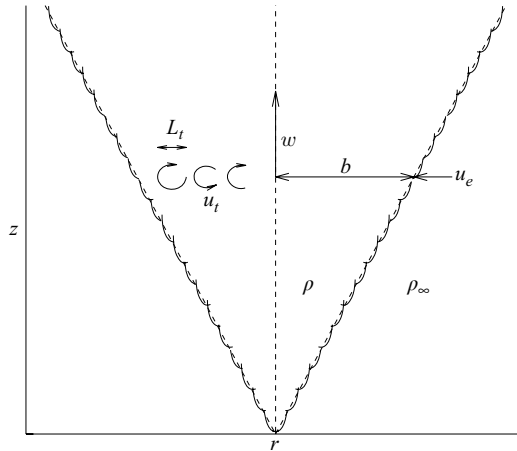


FIGURE 1. A schematic diagram showing a plume with turbulent periphery with: plume radius b , plume velocity w , entrainment velocity u_e , typical eddy length scale L_t and typical eddy velocity scale u_t .

1.1. Present framework

Consider the schematic flow, due to a point source of buoyancy (or momentum), shown in figure 1. The figure shows a rising plume (or jet) with radial coordinate r , vertical coordinate z , characteristic radius b and characteristic vertical velocity w . Furthermore, the ambient fluid has density ρ_∞ whilst the plume has density ρ . Entrainment occurs due to the turbulent eddies arising from the development and breakdown of shear instabilities at the periphery of the ascending plume. At every height within the plume, we assume that we can identify a characteristic radius b , a function of z alone. We then make the assumption of self-similarity for the density $\rho(r, z)$ and vertical velocity $w(r, z)$ in the plume, and so we assume that

$$\rho(r, z) = \rho(z) \left[f_\rho \left(\frac{r}{b} \right) \right], \tag{1.1a}$$

$$w(r, z) = w(z) \left[f_w \left(\frac{r}{b} \right) \right], \tag{1.1b}$$

for some profile functions f_ρ, f_w . For simplicity we assume ‘top-hat’ profiles, i.e.

$$\rho(r, z) = \begin{cases} \rho(z), & r \leq b(z) \\ \rho_\infty(z), & r > b(z), \end{cases} \tag{1.2a}$$

$$w(r, z) = \begin{cases} w(z), & r \leq b(z) \\ 0, & r > b(z). \end{cases} \tag{1.2b}$$

The characteristic scales $\rho(z)$ and $w(z)$ can be thought of as being determined by averaging spatially (at a given height within the plume) and temporally over the turbulent fluctuations associated with the actual entrainment processes. These turbulent eddies will typically have a scale bounded above by the primary Kelvin–Helmholtz billows associated with the shear layer which develops between the plume and the ambient fluid. These billows break down to smaller scales, in general significantly less than b , and the primary physical mechanism of entrainment is through the turbulence within the plume ‘nibbling’ external ambient fluid into the plume itself (see Hunt, Eames & Westerweel 2006).

The entrainment assumption states that the most significant dynamical bulk effect of these turbulent processes, i.e. the flux of ambient fluid into the plume, can be parameterized by a constant, α , relating the effective inflow velocity to the characteristic vertical velocity in the plume. Although there is some evidence that the value of α depends on the buoyancy of the plume, for clarity we assume that it is a constant (also see Hunt & Kaye 2005). There is an implicit assumption in this approach, relevant to the generalization of the entrainment assumption to time-dependent flows. For the averaging to be well-defined, it is necessary for the characteristic time scales of the turbulent eddies to be very much shorter than both the characteristic time scale of the plume at any particular height and the adjustment time of the source strength, t_a . As shown schematically (figure 1), the turbulent eddies have length scale L_t and velocity u_t . Therefore these assumptions are equivalent to $L_t/u_t \ll b/w$, since b/w is the characteristic time scale for the plume evolution, and $L_t/u_t \ll t_a$. These are statements of the assumption that the plume or jet is always turbulent (if the plume or jet is close to a laminar–turbulent transition we might expect the likelihood of pinch-off due to a reduction in driving source conditions to increase due to reduced entrainment). For the assumption of self-similarity it is required that $L_t \ll b$, i.e. the characteristic turbulent length scales are small compared to that of the plume, as is expected on physical grounds.

1.2. Summary of paper

The rest of the paper is organized as follows. In §2 we generalize the governing equations for the evolution of the bulk characteristics of the isolated source to allow for time-dependence, in particular, we make no Boussinesq assumption. In §3 we show that the equations support separable similarity solutions in a homogeneous environment for both plumes and jets with fluxes which increase with height, and decrease with time. In §4 we also demonstrate that these solutions are stable in both space and time to small perturbations, travelling at the local plume (or jet) velocity.

In §5, we consider numerical solutions of the equations where the source conditions for jets and both Boussinesq and non-Boussinesq pure plumes are reduced from an initial to a final value. We find that the jet or plume converges to the time-dependent similarity solution in a transitional adjustment region between a lower region, corresponding to a steady similarity solution determined by the new source conditions, and an upper region corresponding to a steady similarity solution determined by the old source conditions. In §§6 and 7, we draw conclusions, focusing in particular on the relevance of the observed narrowing to potential pinch-off – of weakening plumes or jets – into thermals or puffs in realistic geophysical situations.

2. Derivation of governing equations

Following MTT56, we assume that the flow is axisymmetric with no swirl and that diffusive processes can be ignored. We assume that the radial length scale is smaller than the vertical length scale of the plume or jet and so vertical pressure gradients may be ignored. We derive a self-consistent system of governing equations for a plume or jet under the assumption that density and vertical velocity have a ‘top-hat’ distribution at any given height within the plume.

We identify the edge of the plume or jet with b and suppose that it is entraining fluid horizontally at its edge with some radial velocity $u_e < 0$. In order for the top-hat model to remain self-consistent, it is required that the entrained fluid is instantaneously distributed over the plume’s horizontal area at the given height with the local vertical

velocity. At a given height z and time t , the fluid volume entrainment rate per unit height into the plume or jet is $-2\pi b u_e$, while the mass entrainment rate per unit height is $-2\pi b u_e \rho_\infty$. The fact that the fluid entrained into the plume has zero vertical velocity but must instantly adjust to the local velocity inside the plume constitutes a sink in the momentum equation of strength $2\pi b u_e \rho_\infty w$. Hence within the plume or jet, writing the axisymmetric fluid velocity $\mathbf{u}(r, z, t) = (u_r, w)$, the following volume, mass and momentum equations hold:

$$\nabla \cdot \mathbf{u} = -\frac{2u_e}{b}, \quad \frac{D\rho}{Dt} = -\frac{2(\rho_\infty - \rho)u_e}{b}, \quad \frac{Dw}{Dt} = g \frac{\rho_\infty - \rho}{\rho} + \frac{2\rho_\infty u_e w}{b\rho}. \quad (2.1a-c)$$

We have an additional kinematic boundary condition at the edge of the plume given by

$$u_r|_{r=b_-} = \frac{\partial b}{\partial t} + w \frac{\partial b}{\partial z}, \quad (2.2)$$

noting that this necessarily introduces a discontinuity in u_r at $r=b$ since $u_r|_{b_+} = u_e$ by definition.

We rewrite the mass flux equation (2.1b) in cylindrical polar coordinates, having multiplied through by r and substituting in (2.1a), as

$$\frac{\partial}{\partial t}(r\rho) + \frac{\partial}{\partial r}(ru_r\rho) + \frac{\partial}{\partial z}(rw\rho) = -\frac{2\rho_\infty u_e r}{b}. \quad (2.3)$$

We then integrate (2.3) over $r \in [0, b)$ and apply Leibniz's rule, giving

$$\frac{\partial}{\partial t} \int_0^{b_-} r\rho \, dr - b\rho \frac{\partial b}{\partial t} + b\rho u_r|_{r=b_-} + \frac{\partial}{\partial z} \int_0^{b_-} r\rho w \, dr - bw\rho \frac{\partial b}{\partial z} = -\rho_\infty u_e b. \quad (2.4)$$

Substitution of (2.2) into (2.4) and multiplying through by 2 yields the mass flux equation

$$\frac{\partial}{\partial t}(b^2\rho) + \frac{\partial}{\partial z}(b^2\rho w) = -2\rho_\infty u_e b. \quad (2.5)$$

The buoyancy flux equation is found by rewriting (2.3) and adding and subtracting equal terms to give

$$\begin{aligned} \frac{\partial}{\partial t}[r(\rho - \rho_\infty)] + \frac{\partial}{\partial r}[ru_r(\rho - \rho_\infty)] + \frac{\partial}{\partial z}[rw(\rho - \rho_\infty)] \\ + \rho_\infty r \left\{ \frac{1}{r} \frac{\partial}{\partial r}(ru_r) + \frac{\partial w}{\partial z} \right\} = -rw \frac{d\rho_\infty}{dz} - \frac{2\rho_\infty u_e r}{b}. \end{aligned} \quad (2.6)$$

We substitute for the term in curly brackets using (2.1a) and therefore (2.6) reduces to

$$\frac{\partial}{\partial t}[r(\rho - \rho_\infty)] + \frac{\partial}{\partial r}[ru_r(\rho - \rho_\infty)] + \frac{\partial}{\partial z}[rw(\rho - \rho_\infty)] = -rw \frac{d\rho_\infty}{dz}. \quad (2.7)$$

Integrating (2.7) over $r \in [0, b)$ and applying Leibniz's rule and the kinematic boundary condition (2.2) gives the buoyancy flux equation

$$\frac{\partial}{\partial t}[b^2(\rho_\infty - \rho)] + \frac{\partial}{\partial z}[b^2w(\rho_\infty - \rho)] = -\frac{d\rho_\infty}{dz} b^2 w. \quad (2.8)$$

To find the momentum flux equation we rewrite the vertical Euler equation (2.1c) in conservative form

$$\frac{\partial}{\partial t}(r\rho w) + \frac{\partial}{\partial r}(r\rho u_r w) + \frac{\partial}{\partial z}(r\rho w^2) - wr \left\{ \frac{\partial \rho}{\partial t} + \frac{1}{r} \frac{\partial}{\partial r}(r\rho u_r) + \frac{\partial}{\partial z}(\rho w) \right\} = gr(\rho_\infty - \rho) + \frac{2\rho_\infty u_e wr}{b}. \quad (2.9)$$

We substitute for the quantity in the curly brackets using (2.3), giving

$$\frac{\partial}{\partial t}(r\rho w) + \frac{\partial}{\partial r}(r\rho u_r w) + \frac{\partial}{\partial z}(r\rho w^2) = gr(\rho_\infty - \rho). \quad (2.10)$$

Again, we integrate (2.10) over $r \in [0, b]$ and apply both Leibniz's rule and the kinematic boundary condition (2.3) to get the momentum flux equation

$$\frac{\partial}{\partial t}(b^2 w \rho) + \frac{\partial}{\partial z}(b^2 w^2 \rho) = g[b^2(\rho_\infty - \rho)]. \quad (2.11)$$

This closes the system with (2.5) and (2.8) for b , w and ρ if $\rho_\infty(z)$ is known and u_e is modelled in terms of these variables. Note that the Boussinesq approximation (Boussinesq 1903) has not been made, but corresponds to the distinguished limit $g \rightarrow \infty$, $\rho \rightarrow \rho_\infty$ with the buoyancy force $g(\rho_\infty - \rho)$ remaining constant.

Various assumptions have been made in the literature as to the form of u_e . MTT56 assumed for Boussinesq plumes $u_e = -\alpha w$, with constant α , so that the entrainment into the plume was proportional to the centre velocity of the plume. Ricou & Spalding (1961) observed experimentally non-Boussinesq behaviour with

$$u_e = -\alpha \left(\frac{\rho}{\rho_\infty} \right)^{1/2} w, \quad (2.12)$$

and this is the general form we will use, which is of course consistent with MTT56 in the Boussinesq limit.

Although (2.5), (2.8), (2.11) and (2.12) provide a closed system with top-hat profiles, it is convenient to define a true mass flux, πQ , a true momentum flux, πM , and a true buoyancy flux, πF , where

$$Q(z, t) = b(z, t)^2 w(z, t) \rho(z, t), \quad (2.13a)$$

$$M(z, t) = b(z, t)^2 w(z, t)^2 \rho(z, t), \quad (2.13b)$$

$$F(z, t) = b(z, t)^2 w(z, t) g[\rho_\infty(z) - \rho(z, t)]. \quad (2.13c)$$

It is important to stress that these quantities are valid expressions for both Boussinesq and non-Boussinesq plumes. It follows that

$$w = \frac{M}{Q}, \quad \rho = \rho_\infty \frac{gQ}{gQ + F}, \quad b = \frac{Q}{\sqrt{M\rho}}, \quad g' = g \frac{(\rho_\infty - \rho)}{\rho} = \frac{F}{Q}, \quad (2.14)$$

where g' is the 'reduced gravity'. The buoyancy frequency of the ambient fluid, N , is defined as

$$N^2 = -\frac{g}{\rho_\infty} \frac{d\rho_\infty}{dz}. \quad (2.15)$$

Therefore, the governing equations (2.5), (2.8) and (2.11) together with the entrainment assumption (2.12), the definitions of the fluxes (2.13) and the buoyancy frequency (2.15) give

$$\frac{\partial}{\partial t} \left(\frac{Q^2}{M} \right) + \frac{\partial Q}{\partial z} = 2\alpha \rho_\infty^{1/2} M^{1/2}, \quad (2.16a)$$

$$\frac{\partial Q}{\partial t} + \frac{\partial M}{\partial z} = \frac{QF}{M}, \quad (2.16b)$$

$$\frac{\partial}{\partial t} \left(\frac{QF}{M} \right) + \frac{\partial F}{\partial z} = -N^2 \left(Q + \frac{F}{g} \right), \quad (2.16c)$$

three equations in the three unknowns Q , M and F . The system (2.16) describes the full time-dependent behaviour for a rising† plume with a top-hat profile under the entrainment assumption. Equations (2.16*a*, *b*) rely on conservation of mass and conservation of momentum respectively. It is straightforward to demonstrate that (2.16) has real eigenvalue, w , repeated three times. However, there exist only two linearly independent eigenvectors and so the system is parabolic (see e.g. Whitham 1974). It follows that disturbances to the plume are advected upwards with the local vertical velocity.

For the remainder of the paper, unless otherwise stated, we will consider the ambient fluid to be unstratified, i.e. $N \equiv 0$ and ρ_∞ is a constant.

3. Analysis: similarity solutions

We can identify several classes of separable similarity solutions to equations (2.16). Sections 3.1–3.3 are summaries of existing results, while §§ 3.4–3.6 are new unsteady results.

3.1. Boussinesq plume similarity solutions in an unstratified environment

The steady similarity solutions of a pure plume from a point source identified by Zeldovich (1937) and MTT56 are, in an unstratified environment ($N \equiv 0$), using our notation

$$Q_u(z) = \frac{6\alpha}{5} \left(\frac{9\alpha}{10} \right)^{1/3} F_0^{1/3} \rho_\infty^{2/3} z^{5/3}, \quad M_u(z) = \left(\frac{9\alpha}{10} \right)^{2/3} F_0^{2/3} \rho_\infty^{1/3} z^{4/3}, \quad F_u(z) = F_0. \quad (3.1)$$

At the source $Q_u = 0$, $M_u = 0$ and $F_u = F_0$.

Under the Boussinesq approximation, the similarity solution (3.1) predicts plume radius, plume velocity and reduced gravity to be

$$b_u(z) = \frac{6\alpha z}{5}, \quad w_u(z) = \frac{5}{6\alpha} \left(\frac{9\alpha}{10} \right)^{1/3} \left(\frac{F_0}{\rho_\infty} \right)^{1/3} z^{-1/3}, \quad (3.2a, b)$$

$$g'_u(z) = \frac{5}{6\alpha} \left(\frac{10}{9\alpha} \right)^{1/3} \left(\frac{F_0}{\rho_\infty} \right)^{2/3} z^{-5/3}, \quad (3.2c)$$

with a plume spreading angle of $\tan^{-1}(6\alpha/5)$. In the immediate vicinity of the source, this similarity solution is neither well-defined (as $w \rightarrow \infty$) nor consistent with the averaging assumptions discussed in §1 since $b_u/w_u \rightarrow 0$ as $z \rightarrow 0$. Nevertheless, this solution has proved particularly relevant and useful to the modelling of real plumes, although it is only formally valid for sufficiently large z . Importantly, the velocity

† The case of the descending plume can be straightforwardly realized by reversing the sign of gravity, i.e. replacing g with $-g$. However, the solutions to the governing equations then require the non-Boussinesq plume radius to be complex, rather than real, in some regions, a discussion of which is beyond the scope of the present paper. The profiles of downwards propagating Boussinesq plumes and jets in an unstratified ambient are identical to their upwards propagating counterparts.

increases with buoyancy flux (as $F_0^{1/3}$), but the radius is independent of buoyancy flux (which would be expected on dimensional grounds).

3.2. *Non-Boussinesq plume similarity solutions in an unstratified environment*

If the Boussinesq approximation is not made then for the steady plume solutions (3.1) the plume velocity and reduced gravity are unaffected and the plume radius is given by

$$b_u(z) = \frac{6\alpha z}{5} \left\{ 1 + \left(\frac{z_B}{z} \right)^{5/3} \right\}^{1/2}, \tag{3.3}$$

where

$$z_B = \frac{5}{3} \left(\frac{F_0^2}{20\alpha^4 \rho_\infty^2 g^3} \right)^{1/5}, \tag{3.4}$$

as identified by Woods (1997). The length z_B scales the distance over which non-Boussinesq effects are important. Expansion of (3.3) demonstrates that in the near field the shape of the plume depends critically on z_B , and therefore the buoyancy flux, F_0 , at the origin since

$$b(z) \sim \frac{6\alpha}{5} z_B^{5/6} z^{1/6} + \frac{3\alpha}{5z_B^{5/6}} z^{11/6} + O(z^{7/2}). \tag{3.5}$$

It should be recalled that the vertical pressure gradient was ignored in (2.1c) under the assumption that the radial length scale was smaller than the vertical length scale. Hence, we cannot have strict self-consistency between (3.5) and this assumption close to the source. However, in the far field the shape of the plume becomes less influenced by z_B as

$$b(z) \sim \frac{6\alpha}{5} z + \frac{3\alpha z_B^{5/3}}{5} \frac{1}{z^{2/3}} + O\left(\frac{1}{z^{7/3}}\right). \tag{3.6}$$

Since (3.6) contains no constant term, a virtual origin correction neither can nor needs to be made to correct the far-field Boussinesq predictions for the non-Boussinesq case.

3.3. *Plume similarity solutions in a statically unstable ambient fluid*

Batchelor (1954) considered (as a model of convection) flows where the ambient density increases with height, with a power law of a form equivalent to $N^2 = -N_0^2 z^p$, where N_0 is real and constant, with dimensions $[L^{-p/2} T^{-1}]$, and $p > -8/3$ which ensures that the buoyancy flux increases with height. The steady version of (2.16) with the Boussinesq approximation then supports similarity solutions of the form

$$Q = \frac{32\alpha^2 \rho_\infty}{[2(4+p)(8+3p)]^{1/2}(p+6)^2} N_0 z^{3+p/2}, \quad M = \frac{32\alpha^2 \rho_\infty}{(4+p)(8+3p)(p+6)^2} N_0^2 z^{4+p}, \tag{3.7a, b}$$

$$F = \frac{64\alpha^2 \rho_\infty}{[2(4+p)]^{1/2}(8+3p)^{3/2}(p+6)^2} N_0^3 z^{4+3p/2}. \tag{3.7c}$$

This gives a plume radius, plume velocity and reduced gravity of

$$b = \frac{4\alpha z}{p+6}, \quad w = \left\{ \frac{2}{(4+p)(8+3p)} \right\}^{1/2} N_0 z^{1+p/2}, \quad g' = \frac{2}{8+3p} N_0^2 z^{1+p}. \tag{3.8}$$

In particular, if $p=0$ and hence the statically unstable ambient density has a linear positive gradient ($-N_0^2$) with height, the similarity solution takes the simple form

$$\left. \begin{aligned} Q &= \frac{\alpha^2 \rho_\infty}{9} N_0 z^3, & M &= \frac{\alpha^2 \rho_\infty}{36} N_0^2 z^4, & F &= \frac{\alpha^2 \rho_\infty}{36} N_0^3 z^4, \\ b &= \frac{2\alpha z}{3}, & w &= \frac{N_0 z}{4}, & g' &= \frac{N_0^2 z}{4}. \end{aligned} \right\} \quad (3.9)$$

The velocity does not depend on the buoyancy flux, but rather on the ambient stratification through the parameter N_0 which, for $p=0$, has dimensions $[T^{-1}]$.

3.4. Time-dependent Boussinesq plume similarity solutions

It is possible to identify separable time-dependent similarity solutions to (2.16), with $N \equiv 0$, of the form

$$Q \propto z^{q_z} t^{q_t}, \quad M \propto z^{m_z} t^{m_t}, \quad F \propto z^{f_z} t^{f_t}, \quad (3.10)$$

where q_z, q_t, m_z, m_t, f_z and f_t are unknown exponents chosen to satisfy (2.16). This yields

$$Q = \frac{2\alpha^2 \rho_\infty}{9} \frac{z^3}{t}, \quad M = \frac{\alpha^2 \rho_\infty}{9} \frac{z^4}{t^2}, \quad F = \frac{\alpha^2 \rho_\infty}{9} \frac{z^4}{t^3}, \quad (3.11)$$

which is valid for all positive time. The similarity solution (3.11) predicts, in a Boussinesq fluid, plume radius, plume velocity and reduced gravity given by

$$b = \frac{2\alpha z}{3}, \quad w = \frac{z}{2t}, \quad g' = \frac{z}{2t^2}, \quad (3.12)$$

and so the plume takes the form of a cone as in the steady solution (3.2). It is important to note, however, that the spreading angle of the plume in this time-dependent solution (3.12) is substantially narrower than that found for the steady solution (3.1). Moreover, unlike the steady solution (3.2) the plume velocity predicted by (3.12) increases with height z ; the reduced plume radius can be viewed as a consequence of this.

Since there is no conserved quantity that is independent of time, the predictions provided by (3.12) are the most obvious and natural scalings for the plume radius and velocity, if they are required to depend on both space and time. Interestingly, unlike the MTT56 solutions, but just like the Batchelor (1954) solutions, the plume velocity is not a function of the buoyancy flux, which is itself changing. Consideration of (2.5), (2.11) and (2.12) shows that when the plume is Boussinesq and $w \propto z/t$, it inevitably follows that $b=2\alpha z/3$, irrespective of the particular coefficient of w . This suggests that a spreading angle of $\tan^{-1}(2\alpha/3)$ is a generic feature of plumes where the velocity scales with z (and hence is not dependent on the buoyancy flux). Furthermore, requiring this similarity solution to be consistent with the underlying assumptions of entrainment and self-similarity reduces formally to the requirement of considering sufficiently large z (for b to be adequately large) and sufficiently large t (for the characteristic time scale of the plume, b/w , to be sufficiently large). These are straightforward and natural generalizations of the formal consistency conditions for the classical similarity solutions of MTT56.

It can be seen that the predictions of the time-dependent solution (3.11) are extremely close to the solutions (3.9) that Batchelor (1954) found if N_0 is identified with $2/t$. There is a clear analogy between reducing the buoyancy flux with time at a particular point in space, and entraining fluid in a statically unstable ambient. The additional buoyancy release with height in Batchelor (1954) mimics the effect

of reducing the source buoyancy with time. In both cases the plume’s velocity, w , does not scale with the buoyancy flux which, unlike the steady unstratified case, will increase with height. In the time-dependent flow, fluid at a height $z = z_n$ passed through $z = z_0 < z_n$ at an earlier time, and so naturally the fluid now at $z = z_n$ has a higher buoyancy flux than the fluid now at $z = z_0 < z_n$.

This solution (3.11) requires some time-dependent mechanism by which buoyancy flux can increase with height, unlike Batchelor’s (1954) steady model where this occurs through a statically unstable ambient stratification. As we see in §5, this can also occur through source conditions which decrease with time in a time-dependent flow.

Morton (1959) defined a non-dimensional parameter

$$\Gamma = \frac{5}{8\alpha} \left(\frac{Q}{\rho_\infty} \right)^2 \left(\frac{M}{\rho_\infty} \right)^{-5/2} \left(\frac{F}{\rho_\infty} \right), \tag{3.13}$$

in the present notation, which describes the ‘laziness’ of a plume. At all heights in a pure plume $\Gamma = 1$, the mass, momentum and buoyancy fluxes are in balance. If there is a deficiency of momentum flux, $\Gamma > 1$ and the plume is described as distributed (Caulfield 1991; Caulfield & Woods 1995) or lazy (Hunt & Kaye 2001, 2005). Conversely, if there is an excess of momentum flux compared to pure plume balance, then $\Gamma < 1$ and the plume is described as ‘forced’. For the time-dependent similarity solution (3.11), $\Gamma = 5/6 < 1$, a constant. Therefore the time-dependent solution is forced.

3.5. Time-dependent non-Boussinesq plume similarity solution

The similarity solution (3.11) is equally valid for non-Boussinesq plumes. In this case, however, (3.12) becomes

$$b = \frac{2\alpha z}{3} \left\{ 1 + \frac{z}{2gt^2} \right\}^{1/2}, \quad w = \frac{z}{2t}, \quad g' = \frac{z}{2t^2}, \tag{3.14}$$

which shows the non-Boussinesq plume radius to be both time-dependent and always greater than the Boussinesq plume radius. For early time and large distance from the origin the non-Boussinesq plume radius differs greatly from the Boussinesq plume radius. The velocity and reduced gravity of the non-Boussinesq plume are identical to those of the Boussinesq limit. But as time increases, the non-Boussinesq plume radius tends towards the Boussinesq plume radius for a given height (the density also tends towards the Boussinesq limit).

3.6. Jet similarity solutions

The steady similarity solutions of MTT56, for a pure jet $F \equiv 0$ are

$$Q_u(z) = 2\alpha\rho_\infty^{1/2}M_0^{1/2}z, \quad M_u(z) = M_0. \tag{3.15}$$

The steady jet radius and jet velocity are therefore given by

$$b_u(z) = 2\alpha z, \quad w_u(z) = \frac{M_0^{1/2}}{2\alpha\rho_\infty^{1/2}z}, \tag{3.16}$$

showing $w_u \sim M_0^{1/2}$, with a spreading angle of $\tan^{-1} 2\alpha$. The equations (2.16), with $N \equiv 0$, again support a separable similarity solution of the form

$$Q \propto z^{q_z} t^{q_t}, \quad M \propto z^{m_z} t^{m_t}, \tag{3.17}$$

giving

$$Q = \frac{\alpha^2 \rho_\infty z^3}{9t}, \quad M = \frac{\alpha^2 \rho_\infty z^4}{36t^2}. \tag{3.18}$$

The jet radius and vertical velocity are therefore given respectively by

$$b = \frac{2\alpha z}{3}, \quad w = \frac{z}{4t}, \tag{3.19}$$

with spreading angle $\tan^{-1}(2\alpha/3)$, an inevitable consequence of w being proportional to z . Interestingly, the radius of the jet is the same as for the plume in (3.12), although the velocity of the jet is only half that of the plume.

4. Stability properties of similarity solutions

We wish to establish the stability properties (cf. Caulfield & Woods 1998) of the plume similarity solution given by (3.11) to identify whether plumes with closely related bulk properties will ever converge to these similarity solutions. Therefore we perturb the time-dependent plume similarity solution in the following manner:

$$Q = \frac{2\alpha^2 \rho_\infty z^3}{9t} [1 + \epsilon q(z, t)], \quad M = \frac{\alpha^2 \rho_\infty z^4}{9t^2} [1 + \epsilon m(z, t)], \quad F = \frac{\alpha^2 \rho_\infty z^4}{9t^3} [1 + \epsilon f(z, t)], \tag{4.1}$$

where $\epsilon \ll 1$. Substitution of (4.1) into (2.16) yields, to first order in ϵ , the linear system

$$\begin{pmatrix} 4 & -2 & 0 \\ -1 & 0 & 0 \\ 1 & -1 & 1 \end{pmatrix} 2t \frac{\partial \mathbf{q}}{\partial t} + \begin{pmatrix} 2 & 0 & 0 \\ 0 & -1 & 0 \\ 0 & 0 & 1 \end{pmatrix} z \frac{\partial \mathbf{q}}{\partial z} = \begin{pmatrix} -6 & 3 & 0 \\ -4 & 6 & -2 \\ 4 & -4 & 0 \end{pmatrix} \mathbf{q}, \tag{4.2}$$

where $\mathbf{q} = (q, m, f)^T$. We are particularly interested in perturbations which follow fluid parcels and so we follow perturbations along characteristics travelling with the similarity solution velocity (cf. §2). For such characteristics $2t\partial/\partial t = z\partial/\partial z$. Hence defining $\xi = \log z$, (4.2) reduces to

$$\begin{pmatrix} 6 & -2 & 0 \\ -1 & -1 & 0 \\ 1 & -1 & 2 \end{pmatrix} \frac{\partial \mathbf{q}}{\partial \xi} = \begin{pmatrix} -6 & 3 & 0 \\ -4 & 6 & -2 \\ 4 & -4 & 0 \end{pmatrix} \mathbf{q}. \tag{4.3}$$

Hypothesizing that $\mathbf{q} = \mathbf{q}_0 e^{\sigma \xi}$, where \mathbf{q}_0 is the initial perturbation, we find that σ satisfies

$$(\sigma + 1)(8\sigma^2 + 25\sigma + 12) = 0, \tag{4.4}$$

which has three real negative solutions, which demonstrates that all linear perturbations propagating with the plume velocity will decay in space and time and so we expect to realize the similarity solution at least under some conditions. An identical argument demonstrates that perturbations also decay for the jet similarity solution (3.18), with the equivalent characteristic growth rate of σ given by the quadratic term in (4.4).

Although these similarity solutions appear thus to be, at least conditionally, stable, their relevance needs to be determined by direct solution of the governing equations.

5. Numerical solutions

The governing system of PDEs is parabolic and is solved straightforwardly using the scheme presented in the Appendix A. For both the plume and the jet models, the steady solution corresponding to (3.1) or (3.16) is considered to have existed for all negative time, and at $t=0$ the source conditions are changed.

The system's dependence on both the entrainment coefficient, α , and the ambient density, ρ_∞ , can be removed by introducing the scaled variables

$$\hat{Q} = (\alpha^2 \rho_\infty)^{-2/3} Q, \quad \hat{M} = (\alpha^2 \rho_\infty)^{-1/3} M, \quad \hat{F} = F, \quad \hat{z} = z, \quad \hat{t} = (\alpha^2 \rho_\infty)^{-1/3} t; \quad (5.1)$$

however in the present calculations, for simplicity, α has been set to unity and ρ_∞ has been taken as 1 kg m^{-3} .

5.1. Numerical plume solution

For plume problems, at $t=0$ the buoyancy flux at the origin is reduced from F_0 to F_1 over a time t_a such that

$$F(0, t) = \begin{cases} F_0, & t < 0, \\ f(t), & 0 \leq t < t_a, \\ F_1, & t_a \leq t, \end{cases} \quad (5.2)$$

where $f(0) = F_0$, $f(t_a) = F_1$ and $0 \leq F_1 \leq F_0$. It is assumed that f is a 'well-behaved' arbitrary function.

A new 'steady' plume is established for $t > t_a$ with buoyancy flux F_1 at the origin. The similarity solution for the new 'steady' plume corresponding to (3.1) is the same but with F_0 replaced by F_1 . This leaves the plume radius unchanged in the Boussinesq case with $b = 6\alpha z/5$. In the non-Boussinesq case the plume radius is now given by (3.3) but with F_0 replaced by F_1 . Hence the new plume lies inside the envelope of the old plume.

If it is assumed that the upper region of the plume remains largely unaffected by changes at the source, then the top of the transitional region will be at a height corresponding to a parcel of fluid rising with the original plume velocity, released at time $t=0$. This height is given by

$$z_0 = \left(\frac{10}{9\alpha}\right)^{1/2} \left(\frac{F_0}{\rho_\infty}\right)^{1/4} t^{3/4}. \quad (5.3)$$

The height of the bottom of the transitional region is equivalently given by a parcel of fluid released at $t = t_a$ with a buoyancy flux given by F_1 . This height is given by

$$z_1 = \left(\frac{10}{9\alpha}\right)^{1/2} \left(\frac{F_1}{\rho_\infty}\right)^{1/4} (t - t_a)^{3/4}, \quad (5.4)$$

with the assumptions of entrainment and self-similarity. It follows that the size of the transitional region increases with time. Formal consistency of the time-dependent solutions in this transitional region is thus guaranteed for sufficiently large values of t .

Figure 2 shows the plume shape for a Boussinesq plume with buoyancy flux at the origin described by (5.2). The solution is not sensitive to the precise form of $f(t)$, but for this figure a linear decrease of the form $f(t) = F_0 - (F_0 - F_1)t/t_a$ was used. The buoyancy flux was turned down quickly, with $t_a = 10^{-4}$ s, from $F_0 = 1 \text{ kg m s}^{-3}$

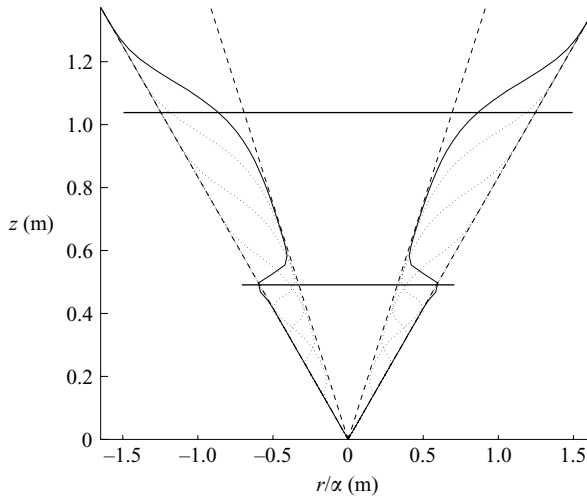


FIGURE 2. The evolution of the plume radius profile for $t = 0, 0.2, \dots, 0.8$ s (dotted) and $t = 1$ s (solid), with $t_a = 1 \times 10^{-4}$ s, $F_0 = 1 \text{ kg m s}^{-3}$ and $F_1 = 5 \times 10^{-2} \text{ kg m s}^{-3}$. The horizontal black lines indicate the expected top, z_0 , and bottom, z_1 , of the narrowing region, at time $t = 1$ s, defined by (5.3) and (5.4). The outer dashed line is the steady $b = 6\alpha z/5$ solution, the inner dashed line is the $b = 2\alpha z/3$ solution corresponding to the transient similarity solution (3.12).

to $F_1 = 5 \times 10^{-2} \text{ kg m s}^{-3}$. The horizontal black lines are the predicted top, z_0 , and bottom, z_1 , of the transitional region at time $t = 1$ s, given by (5.3) and (5.4). The outer dashed lines are the steady Boussinesq plume shape predicted by MTT56, given in (3.1). The inner dashed line is the steady Boussinesq plume shape predicted by the transient similarity solution (3.12), and it can be seen that the plume is attracted to the similarity solution in the transitional region. The buoyancy flux at high levels is much higher than at lower levels, and so in the transitional region there is a vertical increase in buoyancy flux, just as in the Batchelor (1954) model. However, once again the solution converges to the time-dependent similarity solution in this transitional region. It can be seen that the upper and lower regions sit on the steady envelope predicted by (3.1). In the transitional region the lower part of the plume seems to expand outwards a small amount before quickly adjusting to the transient similarity solution. The matching at the upper end of the transitional region is slower but can be seen to be largely centred around the height predicted by (5.3).

The other bulk characteristics of the plume (i.e. velocity, w , and reduced gravity, g') also exhibit three distinct regions of behaviour as shown in figure 3. Far from the source, the velocity and the reduced gravity exhibit the expected power-law behaviour for the steady similarity solutions (3.2) ($w \propto z^{-1/3}$, $g' \propto z^{-5/3}$) associated with the initial buoyancy flux. Similarly, near the source w and g' exhibit the power-law behaviour associated with the steady similarity solutions (3.2) for the final source buoyancy flux. In the transitional region between z_0 and z_1 (defined in (5.3) and (5.4) and marked with horizontal dashed lines in figure 3) w and g' exhibit the scaling associated with the new time-dependent similarity solution (3.12).

Since the numerical solution is in terms of Q , M and F , it is possible to interpret the results in either Boussinesq (figure 2) or non-Boussinesq regimes. Figure 4 is the same solution as in figure 2 but interpreted in a non-Boussinesq regime, with the length scale z_B for the initial plume indicated. It can be seen that the lower region

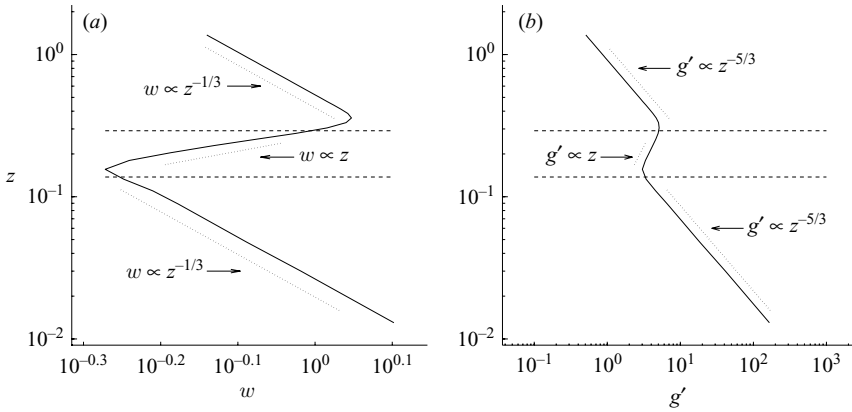


FIGURE 3. (a) A log-log plot of the plume velocity, w , against distance from the source, z , at time $t = 0.2$ s, corresponding to the first dotted line in figure 2. The three regions are shown separated by the heights $z = z_0$ and $z = z_1$, indicated by the horizontal dashed lines. In the three regions the velocity obeys the expected power laws, indicated by the dotted lines. (b) A log-log plot of the reduced gravity, g' , against distance from the source, z , at the same time as in (a). The three regions are shown separated by the heights $z = z_0$ and $z = z_1$. In the three regions the reduced gravity obeys the expected power laws.

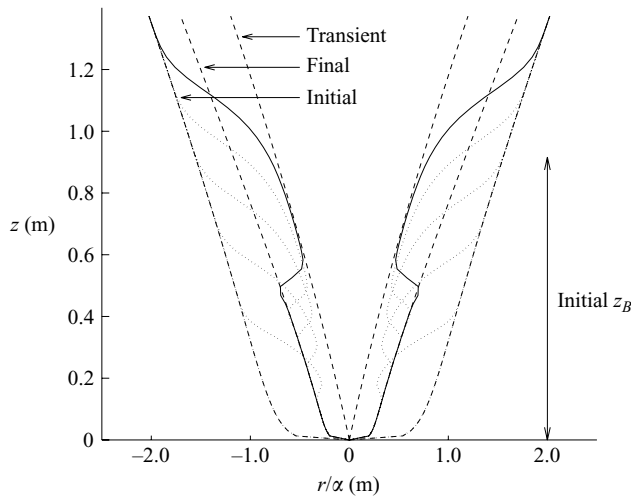


FIGURE 4. The same evolution of the plume radius profile for $t = 0, 0.2, \dots, 0.8$ s (dotted) and $t = 1$ s (solid), with $t_a = 1 \times 10^{-4}$ s, $F_0 = 1 \text{ kg m s}^{-3}$ and $F_1 = 5 \times 10^{-2} \text{ kg m s}^{-3}$ as in figure 2 and additionally $g = 1 \text{ m s}^{-2}$ and $\alpha = 1$. The envelopes given by (3.3) with (3.4) are shown labelled ‘Initial’ and ‘Final’ and the envelope given by (3.14) is shown labelled ‘Transient’.

now lies inside the envelope of the upper region, unlike the Boussinesq case. This is because the length scale z_B is smaller due to the reduced buoyancy flux at the source. The transitional region lies inside both the upper and lower regions. Again the adjustment at the bottom of the transitional region is much faster than at the top of the transitional region. The envelope of the transitional region is time-dependent in the non-Boussinesq case (3.14) and so is only appropriate for a given time.

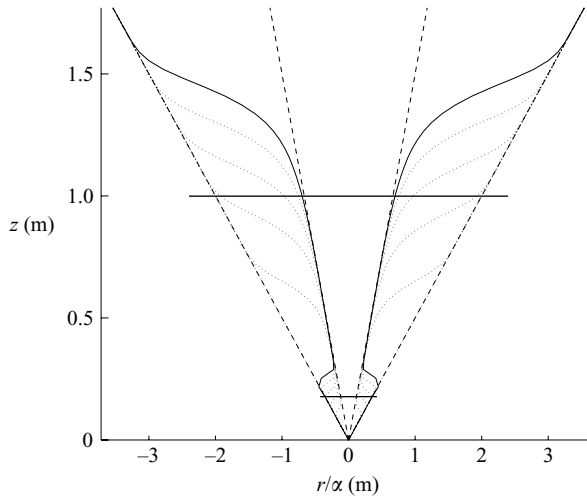


FIGURE 5. The evolution of the jet radius profile for $t=0, 0.2, \dots, 0.8$ s and $t=1$ s (solid), with $t_a = 1 \times 10^{-4}$ s, $M_0 = 1 \text{ kg m s}^{-2}$ and $M_1 = 10^{-3} \text{ kg m s}^{-2}$. The horizontal black lines refer to the expected top, z_0 , and bottom, z_1 , of the transitional region, at time $t=1$ s, given by (5.6).

5.2. Numerical jet solution

At $t=0$ s the momentum flux at the origin is reduced from M_0 to M_1 over a time t_a such that

$$M(0, t) = \begin{cases} M_0, & t < 0, \\ m(t), & 0 \leq t < t_a, \\ M_1, & t_a \leq t, \end{cases} \tag{5.5}$$

where $m(0) = M_0$, $m(t_a) = M_1$ and $0 < M_1 \leq M_0$. It is assumed that m is a ‘well-behaved’ arbitrary function. A new ‘steady’ jet is established with momentum flux M_1 at the origin. The similarity solution for the new ‘steady’ jet corresponding to (3.15) is the same but with M_0 replaced by M_1 . The predicted jet radius remains the same, $b = 2\alpha z$. As before it is expected that the upper and lower regions of the jet will lie on $b = 2\alpha z$ while the transitional region will tend towards $b = 2\alpha z/3$, as given by (3.19).

The heights of the top and bottom of the transitional region for a jet, corresponding to (5.3) and (5.4), are given by

$$z_0 = \frac{1}{\alpha^{1/2}} \left(\frac{M_0}{\rho_\infty} \right)^{1/4} t^{1/2}, \quad z_1 = \frac{1}{\alpha^{1/2}} \left(\frac{M_1}{\rho_\infty} \right)^{1/4} (t - t_a)^{1/2}. \tag{5.6}$$

Figure 5 demonstrates that the jet behaves in a very similar manner to the plume. The upper and lower regions adhere to the steady similarity solution predictions of MTT56, namely $b = 2\alpha z$. The transitional region narrows in to $b = 2\alpha z/3$ as predicted in §3.6. The predictions for the location of the top and bottom of the transitional region are poorer for the jet than for the plume, although they will act as good estimates for the boundaries of the transitional region.

6. Discussion

In this paper we have generalized the bulk plume and jet models of MTT56 to allow for time dependence. The new top-hat averaged system (2.16) allows the modelling

of flows with time-dependent boundary conditions. In §3 it was demonstrated that these systems admit the steady solutions found in MTT56 and also a new class of separable time-dependent similarity solutions. These solutions can be related to the similarity solutions identified by Batchelor (1954) in a statically unstable ambient, with a linear increase in density. In each case the plume velocity increases linearly with height (and independently of the vertically increasing buoyancy flux) and hence the plume radius $b = 2\alpha z/3$. In both cases this linear increase of the plume velocity with height is a natural consequence of the fact that there is no longer a necessity for the plume velocity to scale with a (constant) value of the buoyancy flux. In each instance an alternative time scale exists on which the vertical velocity can depend. The linear stability of these solutions to perturbations travelling at the same speed as the plume or jet velocity was demonstrated in §4.

In both the Boussinesq plume and jet systems it was shown that the narrowing region is bounded by an inner envelope given by $b = 2\alpha z/3$. Since the non-Boussinesq plume radius is always greater than the Boussinesq plume radius, it follows that the non-Boussinesq plume is also bounded by an inner envelope of $b = 2\alpha z/3$. Critically, it also follows therefore that within the confines of the present model, no pinch-off of the plumes or jets can occur. Furthermore, even if the buoyancy flux of the plume or the momentum flux of the jet is reduced to zero, the model predicts that the plume and jet both remain attached to the origin, where the local velocity tends to zero. Once a steady plume or jet is established it is impossible to create complete pinch-off anywhere, within the confines of this model, by reducing the driving source conditions. However, as is apparent in figure 2, when the buoyancy flux is reduced at the source, the interface between the plume and the ambient has significantly shallower slope at the edges of the transitional region between the two steady similarity solutions (i.e. in the vicinity of $z = z_0$ and $z = z_1$). It is plausible that slopes of such a shallow angle may significantly modify the actual entrainment processes. Therefore, pinch-off may well occur due to the breakdown of the extremely simple entrainment assumption at the heart of the time-dependent model presented here. It should also be noted that the time scale, b/w , is intermediate between those of the initial and final steady plumes over most of the transitional region. At the top of the transition region we see a small initial reduction in b/w , but we believe that this is not sufficient to invalidate the assumption that $L_t/u_t \ll b/w$.

In §5 it was demonstrated that these similarity solutions are highly relevant to flows where the source buoyancy flux (for plumes) or source momentum flux (for jets) decreases over finite time from an initial value to a final smaller value. The flow, as shown in figures 2–5, manifests three distinct regions (similar to many other flows in which the driving conditions undergo a transition between two steady states): a far field with the characteristics of the conventional similarity solution of MTT56 given by (3.1) (or (3.16)) with the original buoyancy flux (or momentum flux), a near field with the characteristics of the MTT56 similarity solution with the final buoyancy flux (or momentum flux), and a transitional narrowing region. This transitional region typically approaches closely the new separable time-dependent solution identified in §3.4 and given in (3.11) (or §3.6 and given in (3.18)).

7. Conclusions

Our investigation of the properties of solutions to the time-dependent model problem has several implications for the behaviour of real systems, which, as already mentioned, will typically have time-dependent source conditions. First it appears that,

within the confines of the model presented, plume-like behaviour is very robust to decreases in source conditions (however, in the absence of any experimental evidence, this should be treated with caution). If the source buoyancy flux drops to any non-zero value, we expect plume-like behaviour to persist, with the main observable effect of the reduction in source buoyancy flux being a transitional 'necking' region of reduced but still generally positive spreading rate.

Secondly, for a general mass flux, momentum flux and buoyancy flux, if the source buoyancy flux drops asymptotically to zero at a rate slower than t^{-3} (cf. (3.11), i.e. a theoretical solution can be supported), it appears that at least formally, behaviour of similarity solution type can persist, with a linear rate of spread with height of the plume radius, and a plume velocity increasing with height linearly and decreasing with time. However, it is unclear whether such a solution, with asymptotically decaying source buoyancy flux, can persist in reality. As we have noted, in the immediate vicinity of the source, the entrainment assumption and the assumption of self-similarity are unlikely to be formally valid, and so as the plume weakens it is entirely conceivable that turbulent processes (whose detailed dynamics are outside the scope of these models) may at least intermittently overwhelm the plume-like behaviour and lead to at least intermittent pinch-off. For example since the entrainment process is observed to involve eddies with characteristic length scale bounded above by the plume width, a plume with markedly decreased source buoyancy may be completely disrupted, near the origin, by a turbulent eddy with characteristic length scale comparable with that of the plume at that height. This issue is even more significant where the source buoyancy flux drops to zero in finite time, as then the model predicts zero averaged vertical velocity at the source. This is likely to be inconsistent with real turbulent motions. To understand the behaviour of such systems, or indeed the physical realizability of the predicted model flows discussed here, it will be necessary for example to consider the properties of analogue laboratory experiments.

Conducting complementary laboratory experiments will pose a number of problems. Clearly, ideal plumes and jets cannot be created in a laboratory environment and, as such, some virtual origin problems will be introduced, making direct comparison with the present theory difficult. However, comparison with numerical solutions to the governing system of equations would perhaps be more straightforward. The other significant experimental difficulty will be that unlike steady plume experiments where a simple average over time can be used to calculate the mean plume statistics, many identical experiments would need to be conducted to yield the relevant statistics by ensemble averaging in the temporally varying case considered here.

Finally, the system of equations which governs plumes and jets where the driving source conditions increase is of course identical to (2.16), although there are no attracting similarity solutions for the case of increasing source strength. As discussed in §2, the system is parabolic and all disturbances travel at the local plume velocity. Continuity ensures that the solutions to the system are never multivalued. Hence, whilst disturbances can be, and indeed are in the case of increasing source strength, amplified, no shock can form in the flow. Further discussion of plumes and jets with increasing source conditions is beyond the scope of the present paper.

The authors would like to acknowledge Dr D. M. Leppinen and Dr J. N. McElwaine for some very useful discussions, in addition to the referees who made some extremely valuable comments. M.M.S. was funded under NERC award NER/A/S/2002/00892.

Appendix. Method of numerical solution

In order to solve (2.16) numerically, only perturbations to the steady solutions are considered. Formulating the problem in this way reduces numerical errors as all quantities remain $O(1)$. For brevity the solution of the plume equations will be described. The jet system can be solved using a simplification of the plume method.

Perturbation quantities \tilde{Q} , \tilde{M} and \tilde{F} are defined to be

$$Q(z, t) = Q_u(z)\tilde{Q}(z, t), \quad M(z, t) = M_u(z)\tilde{M}(z, t), \quad F(z, t) = F_u(z)\tilde{F}(z, t), \quad (\text{A } 1)$$

where Q_u , M_u and F_u are as in (3.1).

Defining $\tilde{\mathbf{Q}} = (\tilde{Q}, \tilde{M}, \tilde{F})^T$, it follows from (A 1) and (2.16) that

$$\frac{\partial \tilde{\mathbf{Q}}}{\partial t} = w_u \begin{pmatrix} 0 & -1 & 0 \\ \frac{\tilde{M}^2}{\tilde{Q}^2} & -2\frac{\tilde{M}}{\tilde{Q}} & 0 \\ \frac{\tilde{M}\tilde{F}}{\tilde{Q}^2} & \frac{\tilde{F}}{\tilde{Q}} & -\frac{\tilde{M}}{\tilde{Q}} \end{pmatrix} \frac{\partial \tilde{\mathbf{Q}}}{\partial z} + \frac{w_u}{3z} \begin{pmatrix} 4 \left[\frac{\tilde{Q}\tilde{F}}{\tilde{M}} - \tilde{M} \right] \\ 8\tilde{F} - 3\frac{\tilde{M}^2}{\tilde{Q}} - 5\frac{\tilde{M}^{5/2}}{\tilde{Q}^2} \\ \frac{\tilde{M}\tilde{F}}{\tilde{Q}} - 5\frac{\tilde{M}^{3/2}\tilde{F}}{\tilde{Q}^2} + 4\frac{\tilde{F}^2}{\tilde{M}} \end{pmatrix}, \quad (\text{A } 2)$$

where w_u is the vertical velocity of the plume as defined in (3.2).

In order for all terms to remain $O(1)$ near the origin, the second expression on the right-hand side of (A 2) must vanish as $z \rightarrow 0$. Hence the boundary and initial conditions for the perturbation quantities are given by

$$\tilde{Q}(0, t) = f(t)^{1/3}, \quad \tilde{Q}(z, 0) = 1, \quad (\text{A } 3a)$$

$$\tilde{M}(0, t) = f(t)^{2/3}, \quad \tilde{M}(z, 0) = 1, \quad (\text{A } 3b)$$

$$\tilde{F}(0, t) = f(t), \quad \tilde{F}(z, 0) = 1, \quad (\text{A } 3c)$$

where $f(0) = 1$. This scaling of the time-dependent parts of \tilde{M} and \tilde{Q} relative to \tilde{F} is consistent on dimensional grounds and is a natural characteristic of all the similarity solutions discussed in §3. In the present paper a simple explicit Euler scheme was used.

The solution space is defined to be $(z, t) = [0, z_\ell] \times [0, t_\ell]$. The right-hand side of (A 2) was evaluated at some time t and this was used to time step forward to some $t + \Delta t$. All spatial gradients were calculated using backward differencing, so no information about the boundary was required at $z = z_\ell$ or $t = t_\ell$.

REFERENCES

- BACHELOR, G. K. 1954 Heat convection and buoyancy effects in fluids. *Q. J. R. Met. Soc.* **80**, 339–358.
- BHAT, G. S. & NARASIMHA, R. 1996 A volumetrically heated jet: large-eddy structure and entrainment characteristics. *J. Fluid Mech.* **325**, 303–330.
- BOUSSINESQ, J. 1903 *Théorie Analytique de la Chaleur*. Volume 2. Paris: Gauthier-Villars.
- CAREY, S. N., SIGURDSSON, H. & SPARKS, R. S. J. 1988 Experimental studies of particle-laden plumes. *J. Geophys. Res.* **93**, 15314–15328.
- CAULFIELD, C. P. 1991 Stratification and buoyancy in geophysical flows. PhD Thesis, University of Cambridge, UK.
- CAULFIELD, C. P. & WOODS, A. W. 1995 Plumes with non-monotonic mixing behaviour. *Geophys. Astrophys. Fluid Dyn.* **79**, 173–199.
- CAULFIELD, C. P. & WOODS, A. W. 1998 Turbulent gravitational convection from a point source in a non-uniformly stratified environment. *J. Fluid Mech.* **360**, 229–248.

- HUNT, G. R. & KAYE, N. B. 2001 Virtual origin correction for lazy turbulent plumes. *J. Fluid Mech.* **435**, 377–396.
- HUNT, G. R. & KAYE, N. B. 2005 Lazy plumes. *J. Fluid Mech.* **533**, 329–338.
- HUNT, J. C. R., EAMES, I. & WESTERWEEL, J. 2006 Mechanics of inhomogeneous turbulence and interfacial layers. *J. Fluid Mech.* **554**, 499–523.
- HUNT, J. C. R., VRIELING, A. J., NIEUWSTADT, F. T. M. & FERNANDO, H. J. S. 2003 The influence of the lower boundary on eddy motion in convection. *J. Fluid Mech.* **491**, 183–205.
- MORTON, B. R. 1959 Forced plumes. *J. Fluid Mech.* **5**, 151–163.
- MORTON, B. R., TAYLOR, G. I. & TURNER, J. S. 1956 Turbulent gravitational convection from maintained and instantaneous sources. *Proc. R. Soc. Lond. A* **234**, 1–32 (herein referred to as MTT56).
- RICOU, F. P. & SPALDING, D. B. 1961 Measurements of entrainment by axisymmetrical turbulent jets. *J. Fluid Mech.* **8**, 21–32.
- ROONEY, G. G. & LINDEN, P. F. 1996 Similarity considerations for non-Boussinesq plumes in an unstratified environment. *J. Fluid Mech.* **318**, 237–250.
- TURNER, J. S. 1986 Turbulent entrainment: the development of the entrainment assumption, and its application to geophysical flows. *J. Fluid Mech.* **173**, 431–471.
- WHITHAM, G. B. 1974 *Linear and Nonlinear Waves*. John Wiley & Sons.
- WOODS, A. W. 1997 A note on non-Boussinesq plumes in an incompressible stratified environment. *J. Fluid Mech.* **345**, 347–356.
- WOODS, A. W. & CAULFIELD, C. P. 1992 A laboratory study of explosive volcanic eruptions. *J. Geophys. Res.* **97**, 6699–6712.
- ZELDOVICH, Y. B. 1937 The asymptotic laws of freely-ascending convective flows. *Zhur. Eksper. Teor. Fiz.* **7**, 1463–1465 (in Russian). English transl. in *Selected Works of Yakov Borisovich Zeldovich*, Vol. 1, 1992 (ed. J. P. Ostriker), pp. 82–85. Princeton University Press.